Journal of Coastal Research	15	1	241–260	Royal Palm Beach, Florida	Winter 1999

A One-Dimensional Numerical Model for Storm-Breaching of Barrier Islands

David R. Basco† and Cheol S. Shin‡

†Civil & Environmental Engineering Department
Old Dominion University
Norfolk, VA 23529, U.S.A.

‡Korea Infrastructure Safety Technology Corp. (KISTEC)
Anyang, Dongan-Gu
Kwanyang-Dong 1588-9
Kyunggi-Do, Korea

ABSTRACT

BASCO, D.R., and SHIN, C.S., 1999. A One-Dimensional Numerical Model for Storm-Breaching of Barrier Islands. *Journal of Coastal Research*, 15(1), 241–260. Royal Palm Beach (Florida), ISSN 0749-0208.

A set of numerical models is developed for simulating the four stages of barrier breaching characterized by one horizontal spatial dimension. The SBEACH model (LARSON and KRAUS, 1989) is employed for the first stage of dune/beach erosion. The Lax-Wendroff two-step explicit scheme for Stage II of overland flow is developed to simulate initiation of ocean flood propagation on initially dry barrier islands. The development of the Preissmann implicit scheme for water motion and a forward-time, centered-space explicit scheme for sediment motion in Stage III and IV of storm tidal flow provide a tool to study the volume change and centroid movements of the barrier cross-section above MLLW during various levels of storm activity.

The sensitivity studies show that most sediments are transported landward by large peak storm surge differences between ocean and bay with shorter time lag and longer duration and transported seaward by small peak storm surge differences with longer time lag and shorter storm duration. Grain size significantly affects the movements of the barrier. Median grain size, $D_{50} = 0.4$mm results in maximum volume loss and barrier retreat speed in this study.

Finally, the integrated numerical model is found to produce reasonable results from the various sensitivity tests, which reveal that the numerical model has properly responded to changes of each model parameter. Insight gained from the one-dimensional model will be valuable in the development of a two-dimensional (depth-averaged) model.

ADDITIONAL INDEX WORDS: *Dune/beach erosion, overwash, sediment transport model, tidal inlets, barrier breach.*

INTRODUCTION

Barrier islands protect the bays, lagoons and estuaries that lie behind them. The reduced wave energy environment permits the retention of cohesive sediments and grasses to survive in the tidal marsh areas. About 35 percent of the U.S. coastline is composed of barrier island—bay systems. At many locations, landward migration (transgression) of barrier islands toward the mainland is occurring and is attributed to sea level rise (*e.g.* DOLAN and LINS, 1987).

Two mechanisms for landward migration are (1) rollover due to washover events during storms; and (2) the creation of new tidal inlets and sand trapping in the tidal deltas. LEATHERMAN (1988) has concluded:

> "Overwash is not the dominant process by which most barriers move landward since the amount of sediments transported by this means is too small. (New) inlet formation, when tidal currents cut a channel below sea level moves far greater quantities of sediment into a lagoon over the long term and is the major process for barrier migration" (p.63).

Thus new tidal inlets interrupt the longshore sediment transport processes and play a major role in sediment budgets and shoreline erosion.

96127 received and accepted in revision 20 April 1998.

No generally applicable, semi-theoretical models exist for the prediction of a new tidal inlet along a barrier island coast. This paper summarizes a recent initial step by first considering a one-dimensional approximation of the hydrodynamic and sediment transport processes involved (SHIN, 1996). Dune/beach erosion, overland flow and hydraulic (flood/ebb) flows coupled with sediment transports that create a low profile section across a barrier island are herein defined as a *breach* event. A *new tidal inlet* is therefore defined as a breach event such that the entire low profile section lies *below* the mean lower low water (MLLW) elevation at the conclusion of the storm. Each successive, normal flood-ebb tidal cycle will cause water to flow through the new inlet. Whether the new inlet remains open is a complex question in its own right and beyond the scope of this investigation.

The objective of this study was the development of a set of coupled, one-dimensional, numerical models of the four modeling stages involved, namely: (1) storm surge, wave attack and the dune/beach physics; (2) overwash and overland island flow; (3) storm tidal flooding from ocean to bay; and (4) storm tidal ebbing from bay to ocean. The models employed conservation equations for wave motion, water flow, sediment transport and resulting profile change taking place during the four process stages involved in dune/beach erosion, dune breach and the cutting of a new tidal inlet. These computer models have then provided insight regarding storm energy

levels and durations; barrier island geometry (section volume); phase lags between ocean and bay water levels, and sediment dynamics necessary to produce a break-through event. Knowledge has been gained to help understand why new inlets are created at certain locations along barrier-bay systems during major storm events.

Section 2 summarizes previous attempts at inlet prediction and recent advances in dune/beach response modeling, overland flow, and sediment transport theory that have all aided the development of the coupled models described in Section 3. The numerical modeling details are presented in Section 4. Sandbridge, Virginia is employed as a field test case and the range of independent test variables and example results from the numerical models are summarized in Section 5. The barrier island cross-section volume (area per unit width) above MLLW, its centroid location and speed of movement are the primary dependent variables analyzed in Section 6. Conclusions and recommendations are found in Section 7 where the obvious limitations of the one-dimensional model are also addressed.

The next step is the development of a two-dimensional (horizontal) model. The insight gained from the 1-D modeling effort is proving invaluable in this regard.

STATE OF KNOWLEDGE

Prediction of New Tidal Inlets

In 1986, a conference on tidal inlets was held at the Woods Hole Oceanographical Institute with a compendium of scientific papers edited by AUBREY and WEISHAR (1988). The editors stated in the Preface that this volume provided a broad overview of present day tidal inlet research but failed to address some major questions such as:

> "why are new inlets formed . . . ?"

and,

> "how is climate change going to alter the hydrodynamic balances within tidal inlets and their distribution?"

To these questions we may add a third, namely;

> will global climate and sea level change increase the number and frequency of barrier island breaches and the cutting of new tidal inlets during major storm events?

No generally applicable empirical or semi-theoretical models exist for the prediction of a new tidal inlet along a barrier island coast (SHIN, 1996). PIERCE (1970) qualitatively discussed the conditions under which washover fans or tidal inlets form. Site specific predictions of a new tidal inlet have been made based upon historical records (*e.g.* GIESE, 1978) or using a crude, minimum width-of-island approach (DOLAN, 1985). However, none incorporated the physics of coastal storms, barrier island geometry, and sediment transports within the general laws of mass, momentum and energy conservation to study the potential for island breaching and/or new inlet formation as a break-through event.

Recent, major advances in the physical problem formulation and numerical modeling of (1) dune/beach response to coastal storm events and (2) riverine, mobile-bed and sediment dynamics have now made it possible to solve the barrier island, break-through problem, as summarized below.

Dune/Beach Response Models

For thirty years, a number of dune/beach erosion models have been developed using empirical, analytical and numerical methods (EDELMANN, 1968, 1972; SWART, 1976; DEAN 1976, 1977; VELLINGA, 1982, 1983; MOORE, 1982; KRIEBEL and DEAN, 1984, 1985; LARSON and KRAUS, 1989; STEETZEL, 1993). A recent study (SCHOONEES and THERON, 1995) evaluated ten of the most well-known cross-shore transport models on both a theoretical basis (mainly sediment transport physics) and verification data (morphodynamic response). In their evaluation, the model by LARSON and KRAUS (1989) called SBEACH was classified into the *satisfactory* group for theory because it relies heavily on empirical data. It was also placed in the *best group* category when calculated profiles were compared with observed profile data.

As will be shown below (Section 6) the initial dune/beach profile change *prior* to storm surge overtopping the dune and overland flow across the island, is a relatively minor part of the total breach process.

Mobile Bed Numerical Models and Sediment Transport Formulas

It has long been recognized that the water motion celerities are much larger in absolute magnitude than the celerity for a disturbance at the bed (*e.g.*, DE VRIES, 1965). This has led to decoupling of the hydraulic and sediment equations (CHEN, 1973; DE VRIES, 1973; PARK and JAIN, 1986, 1987). Most applications employ the finite-difference method to first solve for the water surface profile and then to adjust the bed elevation using the sediment continuity equation. This is the uncoupled mode and applicable when changes in bed elevation are very small within each time step in the numerical integration.

Recent advances employ a fully coupled model that distinctly separates the bedload transport at relatively slow propagation speed from the suspended load transport at essentially the water velocity. (see, *e.g.* LYN, 1987; RAHUEL *et al.*, 1989; HOLLY and RAHUEL, 1990; HSU and HOLLY, 1992; CORREIA *et al.*, 1992).

There is no one sediment transport formula that is valid for all ranges of natural conditions (WHITE *et al.*, 1973; BATHURST *et al.*, 1987; VOOGT *et al.*, 1991). CORREIA *et al.* (1992) provide seven options in their model which can be selected by the user for a given set of boundary conditions. For high shear stresses, WILSON (1987) and WILSON and NNADI (1990) have proposed modifications of the classical coefficients for transport rate and friction slope. Similar investigations in the Netherlands for velocities up to 2.7 m/s and fine sand (0.1–0.4 mm) found that the formulas of ENGELUND and HANSEN (1967) and ACKERS and WHITE (1973) over-predicted transport rates by a considerable amount. The engineering formulas of VAN RIJN (1984 a, b, and c) gave the best agreement for the high velocity cases. They have been employed in models for hyper-concentrated, sand-water mixtures (10–50 percent sand concentration by volume) to

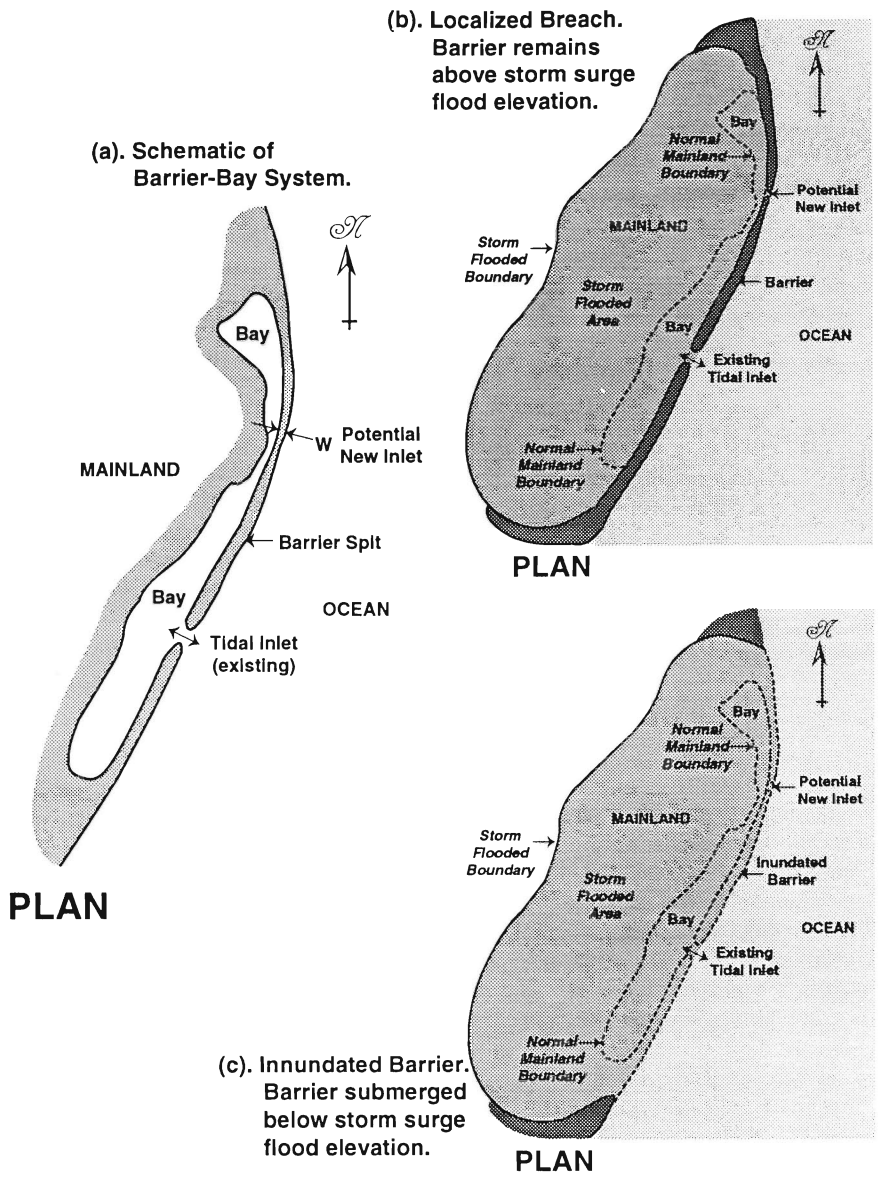

Figure 1. Schematic of Barrier—Bay System.

simulate mixed, subcritical and supercritical flows over an erodible bed during the closure of the Eastern Scheldt in the Netherlands (VOOGT *et al.,* 1991).

ONE-DIMENSIONAL MODEL FORMULATION

General Overview

Dune/beach erosion, wave overwash and hydraulic (flood/ebb) flows can produce a relatively low profile section across a barrier island. Figure 1(a) schematically depicts a barrier-bay system with one existing tidal inlet. A potential new inlet location is also indicated. Many factors determine its location. The coastal orientation, offshore bathymetry and exposure to storm energy are factors; the mainland topography, planform geometry and bathymetry of the bay are factors; the barrier width, elevation, hence cross-sectional volume are factors; and the location of the existing inlet is a factor in that the distance will cause lags in the storm tide amplitude and phase between the ocean and the bay. For example, in Figure 1(a) the distance and narrow restriction in the north end of the bay will create phase lags for both storm flooding and storm ebbing tidal cycles. Storm ebb flows in the northern bay may take a "path of least resistance" to turn a breach into a new inlet at the potential location shown in Figure 1(a). Although only a schematic, the geometry of Figure 1(a) is similar to that present in 1933 for the new inlet formation at Ocean City, Maryland (hurricane) and in 1987 at Nauset Beach, Chatham, Massachusetts (northeaster).

Two simplified modes for break-through events are considered.

Localized Breach

The barrier island generally remains *above* the maximum storm surge flood elevation except at *localized* spot(s) where breaching occurs. The situation is depicted in Figure 1(b) for the same barrier-bay schematic. Storm flood flows create a mainland flooded region and the storm ebb flows return only through the existing inlet and the local breaching location(s). One or more new inlets may form at the end of a storm event. Clearly, flow is concentrated through the localized breach for the entire storm event.

Inundated Barrier

A second possibility exists if the entire barrier island generally becomes submerged below the maximum storm surge flood elevation as depicted in Figure 1(c). The mainland flooded area may be similar but now the early storm ebb flows return across the entire barrier. Eventually the storm ebbs only through the existing inlet and the lowest breaching locations. The return ebb flow covers the barrier until the topography constricts it to the breach location(s). Again, one or more new inlets may form.

One-Dimensional Flows

Free-surface, fluid flows *dominated* by one spatial dimension can be modeled as one-dimensional flows. The most common example is riverine flows where the mean cross-sectional velocity (or volumetric flow rate) and cross-sectional area (or water depth) are the dependent variables of interest as depicted in Figure 2(a). The hydraulic radius characterizes the cross-section and approaches the water depth for "very wide", open channels. In this case, the one-dimensional flow can be considered on a per unit width basis. (see, *e.g.* CHOW, 1957).

For the localized breach case depicted in Figure 1(b), flow across the island is concentrated at one location and generally in one direction as schematized in Figure 2(b). Flow depths are small relative to flow widths so that a unit width "slice" can be considered that extends past the barrier island into the ocean and bay. However, the flows are clearly two-dimensional (horizontal) approaching the breach and the sediment also spreads laterally in these open water regions. A one-dimensional model could be devised assuming radial flow sections and lateral sediment spreading in the open water regions but was not attempted.

The inundated barrier case schematized in Figure 1(c) assumes a wide cross-island flow in one dominant direction as depicted in Figure 2(c). Flows approaching the submerged barrier from the ocean (flood) and the bay (ebb) are clearly also one-dimensional so that the unit width "slice" in open water is still valid for the conservation of mass and momentum for the water and conservation of mass for the sediment. The one-dimensional model described in this paper is valid in this case.

One Dimensional Model Formulation

The breaching process has been divided into four stages.

Stage I—Dune/Beach Erosion

Morphologic changes exhibited by beaches are on a spatial scale of meters and on a time scale of hours for storm events. LARSON and KRAUS (1989) employed a macroscale approach based upon sound, empirical data to develop the beach profile change, numerical simulation model SBEACH. The model was first developed from a large data set of net cross-shore sand transport rates and geomorphic change observed in large wave tanks. It was then verified using high quality field data. A new criterion was developed for predicting when erosional or accretional conditions are present. The model uses this criterion to calculate net sand transport rates (and direction) in four subregions of the nearshore extending from deep water to the limit of wave runup. Wave height distribution is calculated across the shoreface by applying linear wave theory up to the breaking point and then the breaker decay model of DALLY, DEAN and DALRYMPLE (1985a and b) in the surf zone region. Irregular, random wave breaking conditions are included in an upgraded version. Changes in beach profile are calculated from the distribution of cross-shore sand transport rate and the equation of mass conservation of sand. All sediment transport and beach profile changes are shore normal, hence in one horizontal space dimension.

Stage II—Overwash/Overland Flow

Continued rising water level accompanied by irregular wave runup will eventually create landward directed flows across the barrier when the water levels exceed the eroded dune crest elevation. Morphologic change is over spatial scales of meters but now on a time scale of minutes that depends on barrier width and the rate of hydrograph rise during the storm event.

The shallow-water equations of free-surface, unsteady, open-channel flow (DE SAINT VENANT, 1871) form the basis of most mathematical models of riverine hydraulics. They assume a hydrostatic pressure distribution and that the dependent variables, velocity and water depth are continuous, differentiable functions. However, in Stage II at certain locations due to shallow water depths and steep slopes, the velocity and water depth may become discontinuous (*i.e.* hydraulic jump or bore). In this case, the differential equations describing the water flow must be expressed in conservation form (*e.g.* ABBOTT and BASCO, 1989). In vector notation they become

$$\frac{\partial \bar{V}}{\partial t} + \frac{\partial \bar{F}(\bar{V})}{\partial x} = \bar{G}(\bar{V}) \tag{1}$$

with

$$\bar{V} = \begin{bmatrix} h \\ q \end{bmatrix} \tag{2}$$

$$\bar{F}(\bar{V}) = \begin{bmatrix} q \\ \frac{q^2}{h} + \frac{1}{2} g h^2 \end{bmatrix} \tag{3}$$

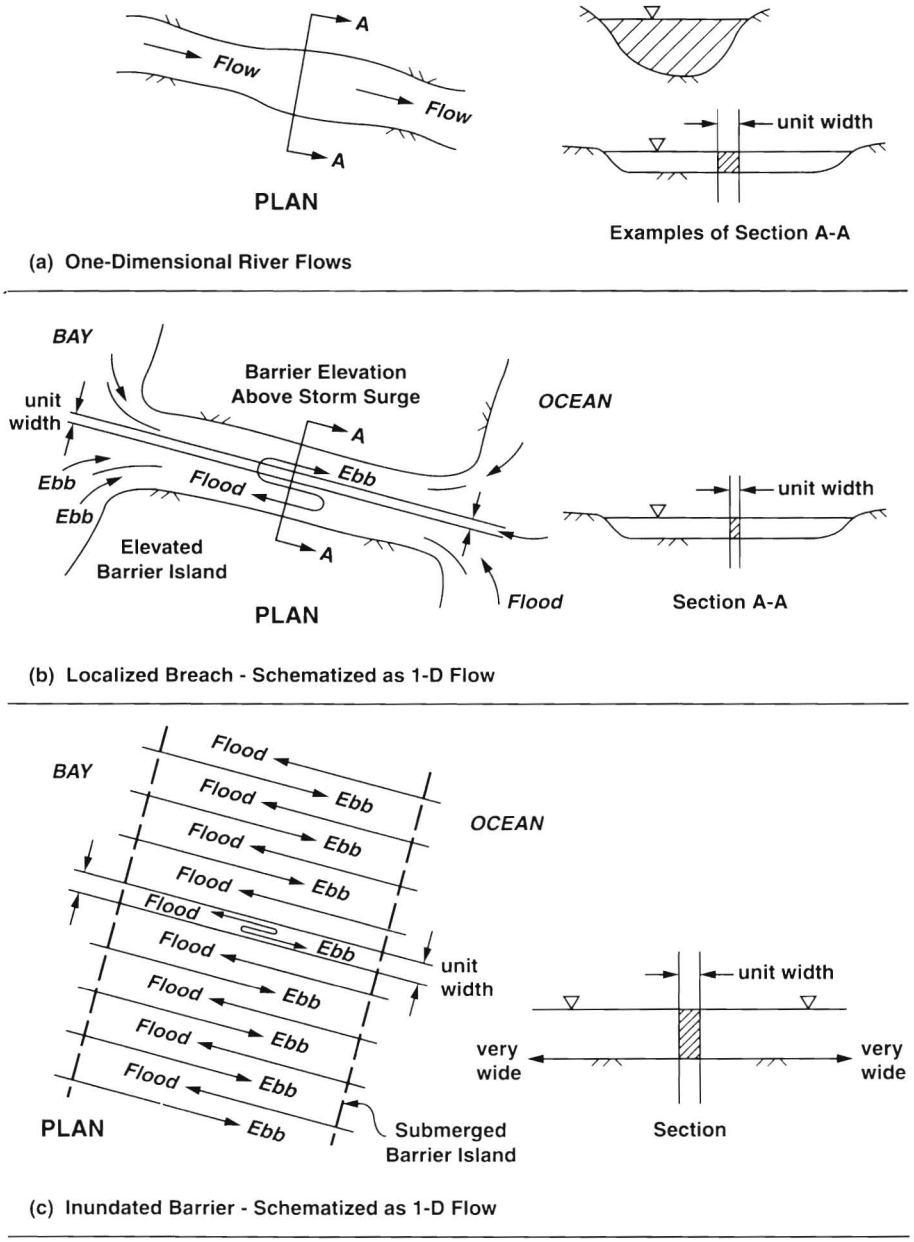

Figure 2. One-Dimensional Flows. (a) rivers, (b) localized breach, (c) inundated barrier.

$$\bar{G}(\bar{V}) = \begin{bmatrix} 0 \\ gh\dfrac{\partial Z}{\partial x} - ghS_f \end{bmatrix} \tag{4}$$

$$S_f = \frac{q|q|}{C_c^2 h^3} \tag{5}$$

$$C_c = 18 \log\left[\frac{12h}{k_s}\right] \tag{6}$$

where h(x,t) is the local water depth; q(x,t) is the volumetric flowrate per unit width; z(x,t) is the elevation of the bed referenced to an arbitrary datum; S_f is the friction slope; C_c is the Chezy boundary resistance coefficient; k_s is the hydraulic roughness of the movable bed; and g is the acceleration of gravity.

During the extremely short time period for Stage II (generally less then 10 minutes) wave overtopping, overwash and overland flows will generally *smooth-out* the pre-storm, barrier profile landward of the dune crest. Consequently, profile change is modeled as a simple diffusion process with no advection. Stage II is to basically develop

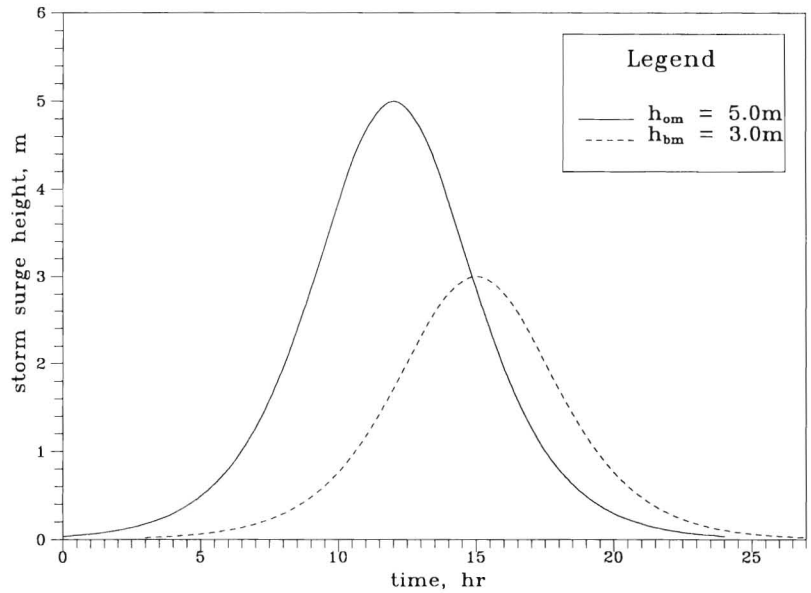

Figure 3. Example Storm-surge Hydrographs (h_{om}=5m, h_{bm}=3m, t_{lag}=3 hrs).

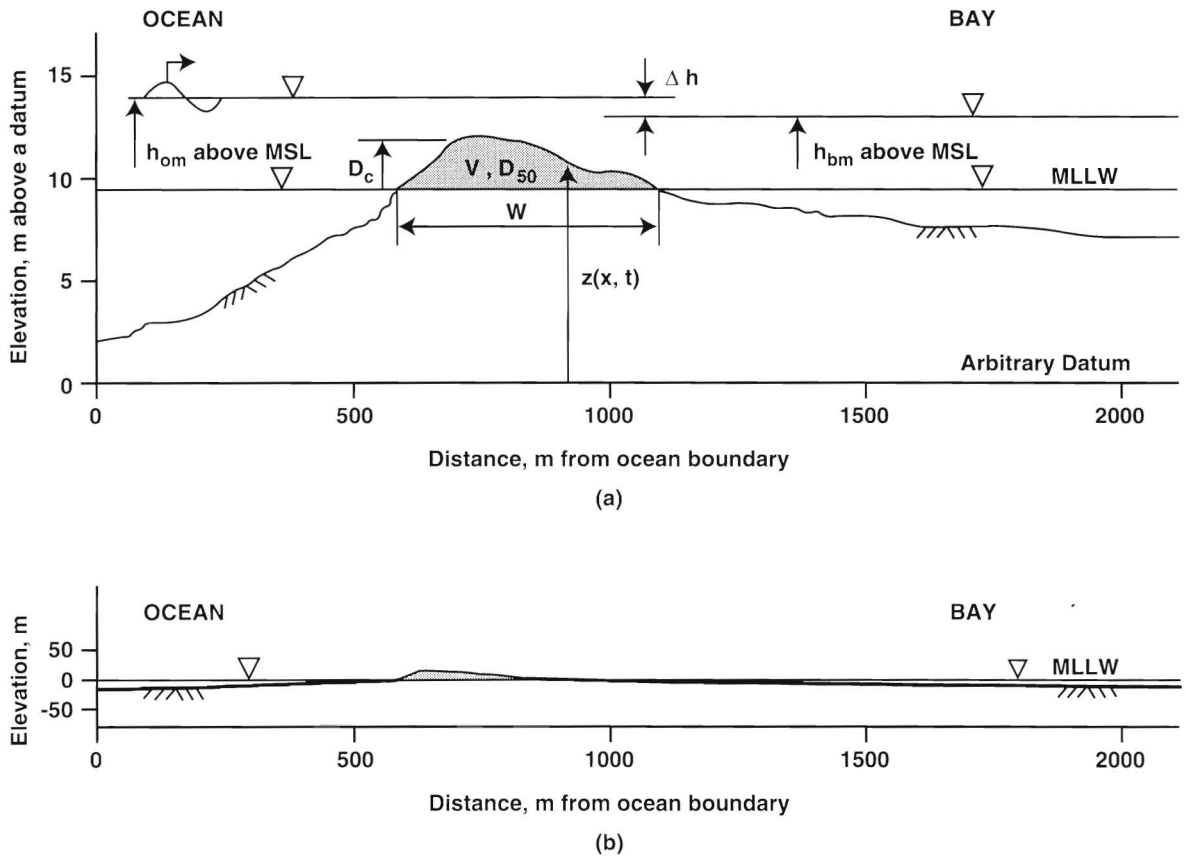

Figure 4. Schematic Representation of Key Independent Variables for a Typical Sandbridge, Virginia Cross-Section (a) distorted scale and (b) undistorted scale.

the *initial conditions* of water motion and bathymetry for the subsequent Stage III.

Stages III and IV—Storm Tides

Continued rising water level in the ocean relative to water level in the bay will produce water flow from ocean to bay (flooding, Stage III). Eventually, the water elevation (level) difference between the bay and ocean reverses so that the water motion changes direction to become ebbing flows (Stage IV) from bay to ocean. Water wave oscillatory motions are considered secondary to advection dominated processes in these stages and are neglected.

Because of the deeper water depths and flatter (smoothed) barrier slopes, the mean flow velocity, u(x,t), found simply from

$$u(x, t) = \frac{q(x, t)}{h(x, t)} \tag{7}$$

and water depth, h(x,t) are now the dependent variables calculated. The non-conservation (Eulerian) form of equations (1)–(5) are employed and a control function introduced in the nonlinear, advection term to handle some cases when mixed-type flows (sub- and super-critical) occur. The technique employed is described by HAVNO and BRORSEN (1986) whereby the nonlinear advection term in the momentum equation is reduced (or suppressed) by a control function, CF defined as

$$CF = \begin{cases} 1 - F_r^2, & F_r < 1 \\ 0, & F_r > 1 \end{cases} \tag{8}$$

where;

$$F_r = \frac{u}{\sqrt{gh}}, \quad \text{the local Froude number}$$

By this means it is possible to maintain a sub-critical flow characteristic structure and data structure over the whole domain of the solution, including sub-domains of supercritical flow. The dominance of the resistance term for small depths also means that suppression of the nonlinear advection term (Fr>0) will have little effect on the results.

The water depth and velocity found from the conservation of water mass and momentum equations are then used to find the local sediment transport rate, q_t. Transport of sediment particles by the flow of water is found as the sum of the bed-load transport rate, q_b, and the suspended-load transport rate, q_s. The fraction of each depends on the grain size of the bed materials and the flow conditions. The methods developed by VAN RIJN (1984a & b) compute the bed-load transport as the product of the saltation height, particle velocity and the bed-load concentration and computes the suspended-load as the depth-integration of the product of the local concentration and flow velocity.

Predictive capabilities of the sediment transport formulas of ENGELUND and HANSEN (1967), ACKERS and WHITE (1973) and VAN RIJN (1984b) at high velocities were investigated by VOOGT *et al.* (1991). The method of VAN RIJN yielded the best results when compared with field measurements for high velocities in the range of 1–3 m/s and bed materials ranging from 0.1–0.4mm. In addition, predicted transport rates from VAN RIJN (1984b) were less sensitive to the Nikuradse bed roughness, which is difficult to estimate under tidal flows. The VAN RIJN (1984b) formulas were employed for computation of the sediment transport rate in this study.

In natural channels, sediment motion is three-dimensional. If we assume that net deposition or erosion between two neighboring sections is uniformly distributed longitudinally (*i.e.*, across the barrier) and per unit width, than the three-dimensional nature can be simulated in a one-dimensional model (MAHMOOD and YEVJEVICH, 1975). The 1-D, sediment continuity equation per unit width (all lateral inflow of sediment assumed zero) is:

$$(1 - p)\frac{\partial Z}{\partial t} + \frac{\partial}{\partial t}(C_s h) + \frac{\partial q_t}{\partial x} = 0 \tag{9}$$

where C_s is the sediment concentration by volume; q_t is the total transport rate for combined bed- and suspended-load, transport; and p is the porosity of bed materials. In riverine flows, the time variation of C_s is very small (MAHMOOD and PONCE, 1976; PONCE *et al.*, 1979; LYN, 1987) and we shall also neglect it here. Equation (9) becomes

$$(1 - p)\frac{\partial Z}{\partial t} + \frac{\partial q_t}{\partial x} = 0 \tag{10}$$

and is employed to determine the corresponding variation in bottom profile, Z(t) for storm tidal flooding (Stage III) and ebbing (Stage IV) conditions. The separation of the model into these two stages helps to provide insight into the physical processes involved.

In summary, the wave, water flow and sediment processes involved in a barrier breach are divided into four modeling stages, namely: (1) wave attack and dune/beach physics; (2) overwash and overland island flow; (3) storm tidal flooding from ocean to bay; and (4) storm tidal ebbing from bay to ocean. Conditions and equations for a one-dimensional model are presented that require *linking* of the four modeling stages and solution by numerical methods as described in the next section.

NUMERICAL MODELS

Because of the extensive number of dune/beach numerical models available, we simply apply the one developed by LARSON and KRAUS (1989) called SBEACH for Stage I. For the other three stages, we have employed the finite-difference method and developed our own numerical models of the applicable conservation equations and sediment transport formulas as described below. Initial and boundary conditions are discussed later.

Stage I—Dune/Beach Erosion

The SBEACH model consists of three modules to consecutively calculate wave height distribution, net cross-shore sediment transport rate and resulting profile change for each time step.

The wave height distribution computation across the initial profile begins at the seaward end and proceeds onshore through a simple explicit scheme of the wave energy flux bal-

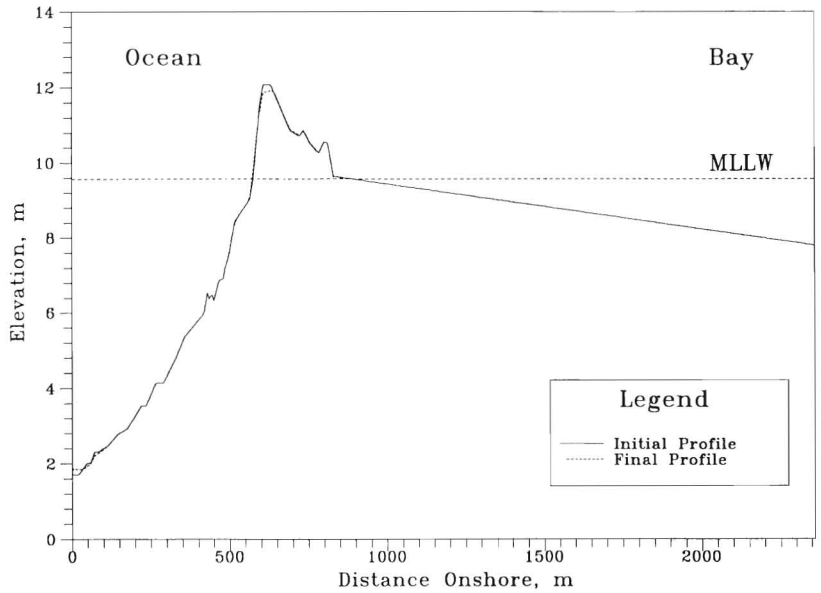

Figure 5. SBEACH Results for h_{om}=5m, H_{mo}=5.54m, T_p=15.25s.

ance equation. At each time step, a check is made to determine if wave breaking has occurred, and hence if additional energy dissipation is required in the model. Profile change is then calculated from the explicit, finite-difference analog of Equation (10) using the net transport rate averaged over the lower and upper time levels.

The concept of avalanching as discussed by ALLEN (1970) is included in a subroutine to account for transport induced by slope failure. Dune overwash in the landward direction is also simulated in the SBEACH model. For complete details see LARSON and KRAUS (1989) and LARSON *et al.* (1990).

Stage I "ends" when the water level in the rising, ocean storm surge hydrograph exceeds the eroded dune crest elevation for the next time step in the simulation. Water wave amplitude oscillations, wave overwash and wave set-up are neglected in this initial, simplified simulation of the physical processes. Oscillatory wave motions are neglected in all subsequent stages because water advection processes dominate.

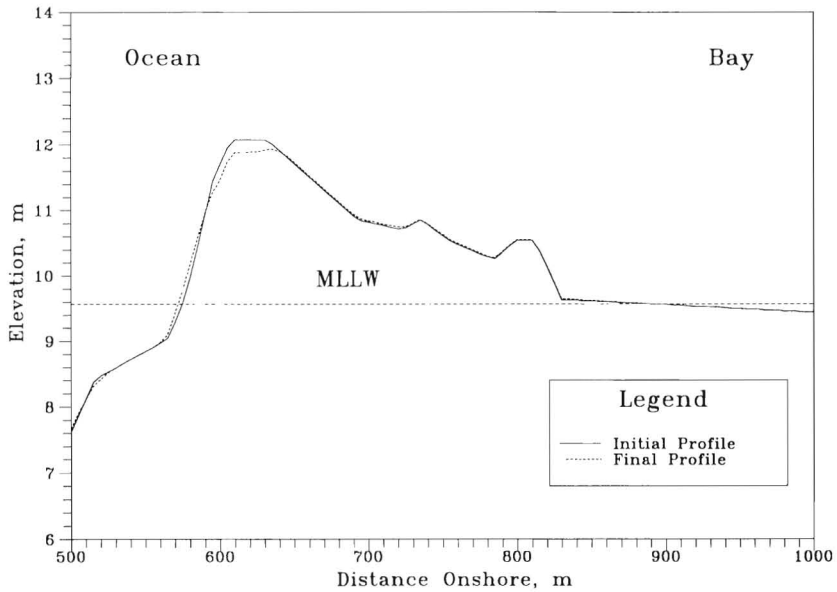

Figure 6. Zoomed Profiles for h_{om}=5m, H_{mo}=5.54m, T_p=15.25s.

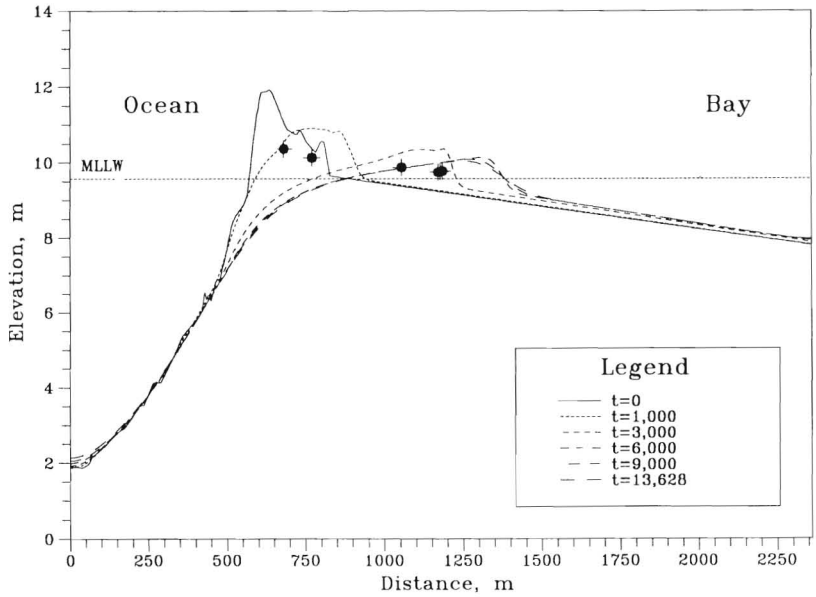

Figure 7. Bed Elevation Changes with Centroids of the Dune above MLLW. (h_{om}=4.0m, h_{bm}=3.0m, t_{lag}=1hr, D_{50}=0.3mm).

Stage II—Overwash/Overland Flow

The conservation forms of the water mass and momentum equations are numerically integrated using the LAX-WENDROFF (1960) two-step, explicit, finite-difference scheme. The first step over one-half time interval, Δt uses the LAX (1954) operator to solve equations (1)-(6) and find values of h and q at staggered grid locations at the intermediate time level. The second step employs a "leap frog" operator with the initial conditions and intermediate time step results to compute h, q values at staggered grid locations for the next time step. It is called "leap frog" operator because some intermediate grid values are not employed in the computation (LAX and WENDROFF, 1960). It is second-order accurate in truncation errors but is also amplitude dissipative for higher wave numbers and therefore often used to model flows with moving shocks and discontinuities. (RICHTMYER and MORTON, 1967; ABBOTT and BASCO, 1989).

The RICHTMYER (1963) version of the LAX-WENDROFF two-step scheme employs a numerical filtering device at alternating time steps to add a small amount of additional dissipation. It is also used in our model to suppress nonlinear instabilities in a controlled manner which come from the initially small water depth (h = 0.03m), base flowrate and abrupt changes in bed profile that produce complex flow situations (*i.e.,* hydraulic jumps and bores) at certain locations over the computational domain.

Subcritical flows require the specification of one-point boundary data (q or h) at each boundary for a unique solution (ABBOTT, 1966). In this study, water depths, h are specified as boundary conditions at both ends of the one-dimensional model. However, the LAX-WENDROFF (1960) two-step scheme requires specification of both q and h at the inflow boundary. To determine the additional boundary value of q, the method-of-characteristics was employed that included taking into account the local bottom slope and shear. For further details see SHIN (1996) and ABBOTT and BASCO (1989, p.229).

The LAX-WENDROFF two-step explicit scheme is numerically stable for Courant numbers less than or equal to one. (RICHTMYER and MORTON 1967). This imposes a limit on the size of the time step, Δt. Maximum values of q and h were found from preliminary tests to insure that all subsequent computations were made with Δt safely below the time step limit.

Prior to the water flow calculations described above, the bed profile was numerically "smoothed" as a simple, local diffusion process with no advection. Volume was conserved across the barrier profile. For the relatively small time required for Stage II, these calculations basically developed the *initial conditions* (water motions and bottom profile) for the subsequent Stages III and IV of the barrier breach model.

Complete numerical details for Stage II are in SHIN (1996).

Stages III and IV—Storm Tidal Flood and Ebb Flows

The Eulerian forms of the water conservation equations (1) to (6) have been numerically integrated using the implicit, compact, finite-difference algorithm called the PREISSMANN (1961) scheme. This scheme has been extensively studied (ABBOTT and BASCO, 1989) and is routinely employed for flood forecasts by the National Weather Service (FREAD, 1974).

Now, the water depth, h(x,t) and the mean velocity, u(x,t) are the dependent flow variables and both calculated for all grid points across the solution domain. The implicit, Preissmann operator generates a penta-diagonal matrix that can be reduced to tri-diagonal form for efficient solution by the "double-sweep" solution (Thomas algorithm) technique. It

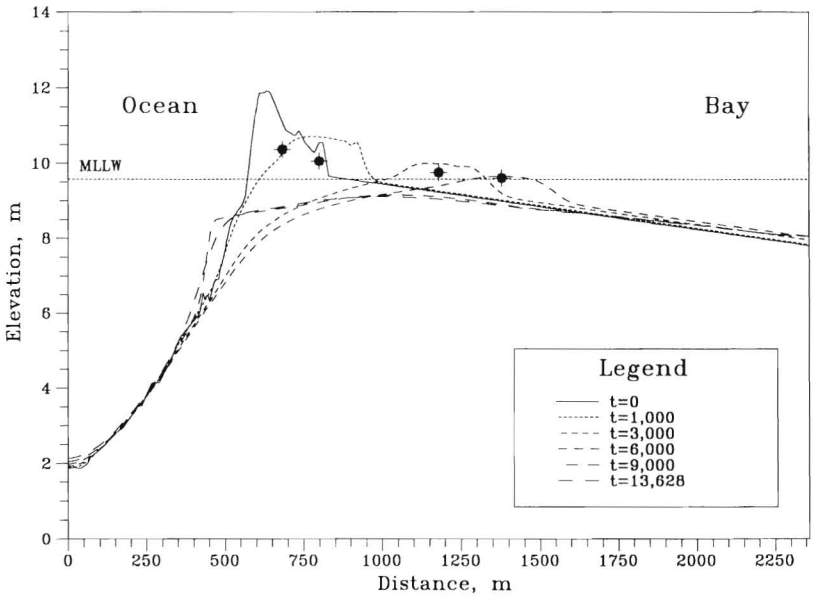

Figure 8. Bed Elevation Changes with Centroids of the Dune above MLLW. (h_{om}=4.0m, h_{bm}=3.0m, t_{lag}=3hr, D_{50}=0.3mm).

employs a weighting coefficient for splitting all space derivatives between the given and next time step level, Δt. If the weighting coefficient is 0.5, the scheme is unconditionally stable with no amplitude errors for any Courant number or Froude number. When the Courant number is one, the scheme also has no phase errors and therefore is numerically exact and equivalent to the method of characteristics. This has been confirmed by a formal truncation error analysis (HILL, 1981) and linear stability analysis of the Preissmann algorithm (BASCO, 1977). For practical applications with bottom slopes and bed shears, the weighting coefficient is usually taken as greater than 0.5 to add a slight amount of numerical dissipation for the higher wave numbers. See also LIGGETT and CUNGE (1975), ABBOTT (1979), CUNGE *et al.* (1980), and ABBOTT and BASCO (1989) for more information on the Preissmann scheme for numerical modeling for river and estuary hydrodynamics.

Once the water depths and velocities at the new time level are known, the sediment transport rates for bed- and suspended-loads are computed from the formulas of VAN RIJN (1984a & b). These loads are combined as the total sediment load and then used in equation (10) to find the local bed elevation change, ΔZ for the time step, Δt. A simple, forward-in-time, centered-space (FTCS) explicit, finite-difference scheme on the same computational grid (as the water motion calculation) is employed. Under rapidly varying flow conditions, *e.g.* across the dune crest, wiggle instabilities of Z(x) grow in time and eventually become unstable. To suppress these wiggles, a numerical filter is again employed at alternative time steps to add a small amount of local "dissipation", *i.e.* to remove the high wave number wiggles. As discussed below, extensive volume conservation calculations proved that no mass was lost in the process. Time steps for the sediment mass conservation equation were again limited by the Courant condition for this FTCS, explicit scheme. However, the celerity (unknown) of the sediment "wave" is very small so that the time step employed for the water motion computation governs.

These numerical methods are employed for both Stages III (flooding) and Stage IV (ebbing) conditions. Separation is only for insite into the directions of sediment transports and barrier volume changes that result.

Initial and Boundary Conditions

Initial water depths over the computational domain are calculated from the initial beach and bay bathymetric data and topographic map of the barrier elevations relative to an arbitrary datum. To make all water depths positive, the arbitrary datum is taken below the seaward depth where no further sediment transport is anticipate. This is typically the "closure depth" employed in most sediment budgets of the coast (HALLERMEIER, 1981).

The key ocean and bay boundary conditions are the storm surge hydrographs. For this study we employ synthetic hurricane storm hydrographs that are analytically described as inverse, squared, hyperbolic functions; namely:
For Ocean

$$h_o(t) = d_o + h_{om}\frac{1}{\cosh^2\left[\frac{2\pi(t - T/2)}{T}\right]} + \sum_{t=0}^{T}\Delta z_1 \qquad (11)$$

For Bay

$$h_b(t) = d_b + h_{bm}\frac{1}{\cosh^2\left[\frac{2\pi(t - \tau - T/2)}{T}\right]} + \sum_{t=0}^{T}\Delta z_{JJ} \qquad (12)$$

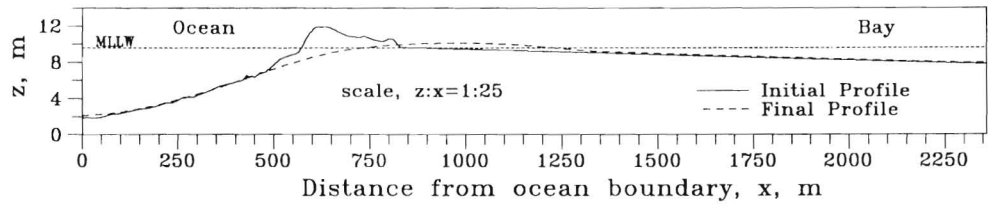

Figure 9. Bed Elevation Changes in Stage III/IV. (h_{om}=4.5m, h_{bm}=4.0m, t_{lag}=1hr, D_{50}=0.3mm).

where d_o and d_b are the initial ocean and bay boundary water depths defined below the design stillwater level (DSWL); $h_o(t)$ and $h_b(t)$ are the water depths at the ocean and bay boundaries, respectively; h_{om} and h_{bm} are the peak ocean and bay storm surge heights respectively; T is the duration of the storm and τ is the lag time between peak storm surges in the ocean and bay. In addition,Δz_1 and Δz_{jj} are the bed level differences calculated each time step, Δt that may occur at the ocean and bay boundaries, respectively. Hence, water depths are adjusted from the cumulative bed level differences for both boundaries.

The key variables are h_{om}, h_{bm} and τ. Figure 3 is an example showing a 24 hour storm surge hydrograph for both ocean (solid) and bay (dotted) with a 3 hour time lag. During Stage III, flooding occurs due to the positive hydraulic head difference, Δh from ocean to bay. At about 15 hours, Stage IV, ebbing begins due to the negative head differential. Stages I and II (not shown) begin at zero time and when the ocean storm surge elevation exceeds the eroded, dune crest elevation, respectively. Note that the maximum head differential between ocean and bay producing the largest velocities and sediment transports depends upon all three independent variables, h_{om}, h_{bm} and τ.

For the sediment continuity equation, we employ Newmann type (gradient) boundary conditions at both boundaries. The boundary condition can naturally adjust to any small quantities of sediment reaching the boundary. Tests with Dirichet type (constant value) boundary conditions were made and these produced numerical oscillations at the boundaries.

NUMERICAL MODEL TEST RESULTS

Test Case—Sandbridge, Virginia

At distorted scales, Figure 4(a) taken from actual field measurements at Sandbridge, Virginia, depicts a typical barrier island profile. The barrier section width, w is about 300m and elevation of the dune crest, D_c is 2.07m above mean sea level (MSL). The barrier section volume, V above mean lower low water (MLLW) tidal datum must be spread laterally in both directions for a breaching event. At undistorted scales, Figure 4(b) presents a true perspective of the relatively thin barrier volume involved.

Figure 4(a) also serves as a definition sketch. An arbitrary datum is chosen as zero elevation so that the ocean boundary water depth is greater than the "closure depth" for wave sediment transport at this location (HALLERMEIER, 1981). The MLLW designation is from the NOS tide tables. Storm surge levels are related to NGVD (1972 adj.) and the City of Virginia Beach (Sandbridge subdivision) vertical datum is NGVD (1929) which is labeled MSL.

Table 1. *Summary of representative storm surge levels, wave heights and periods.*

Return Period in Year	100	350	500	800	1,000
h_{om}, m	3.0	3.5	4.0	4.5	5.0
H_{mo}, m	5.08	5.20	5.32	5.45	5.54
T_p, sec	14.31	14.54	14.78	15.01	15.25

Range of Test Variables Employed

Numerical simulations have been conducted for various cases depending on the (1) ocean and bay peak storm-surge levels (3.0–5.0m); (2) various time lags (0–6hr) between maximum ocean and bay storm-surge elevations; (3) sediment median diameters (0.1–1.0mm), and (4) storm durations (12–48hr). Five different storm-surge levels were selected from available probability of exceedance curves (U.S. ARMY 1989) with related wave heights taken from annual, cumulative wave height distribution curves for this region (LEFFLER *et al.*, 1993). Wave periods were computed using the assumption that the local wave steepness (H_{mo}/L) is constant for all waves, where L is the local wave period. The number of variables derived for each energy level is shown in Table 1.

Example of Test Results

Consider as an example, the case for h_{om} = 5m, H_{mo} = 5.54m, T_p = 15.25s, 0.3mm sediment, zero time lag and a 24 hr duration storm. A simulation result is shown in Figures 5 for the initial (solid) and final (dotted) profiles. Figure 6 presents the same results for the barrier island cross-section at an expanded (zoomed) scale.

For Stage I, no wave action is represented in the bay so that no sediment transport takes place there. The simulation time for Stage II is about ten minutes and can be extended depending on the stability condition of the numerical scheme under given storm surge levels. A space step of ten meters and time step of four seconds were chosen for Stages III and IV. The simulation stops when the flow depth becomes smaller than an initial, base flow depth of approximately 0.03m at

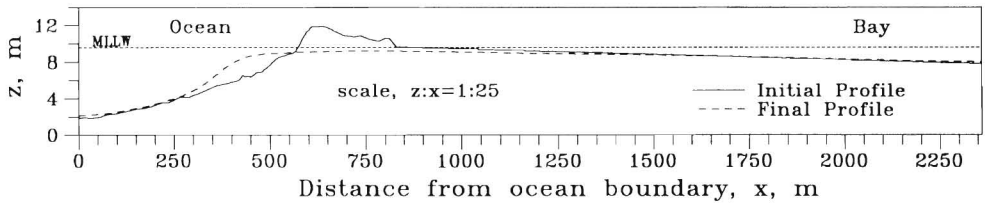

Figure 10. Bed Elevation Changes in Stage III/IV (h_{om}=4.5m, h_{bm}=4.0m, t_{lag}=2hr, D_{50}=0.3mm).

the eroded dune crest. This prevents numerical instability for a zero depth flow condition.

Figure 7 displays intermediate time step results (t = 0, 1000, 3000, etc. time step) with the barrier island movement shown by the centroid positions (black dots) above MLLW. These example results are for a different set of variables (h_{om} = 4m, h_{bm} = 3m, t_{lag}= 1 hour) and Figure 8 shows the effects of a longer, 3 hr time lag on the results. Again, Figures 7 and 8 are plotted at a highly distorted scale (1:125). These same results (initial and final profiles) are also presented as Figures 9 and 10, respectively for a 1:25 distortion. In one case (Figure 9, 1 hr lag) the flattened dune is found on the Bay side of the barrier whereas in the second case (Figure 10, 3 hr lag) the final profile shows a large sand volume seaward of the original dune position. Model sensitivity tests for various time lags, sand diameters and storm durations were conducted, as described below.

Figure 11 is an example of how the water depth (dotted) and water velocity (solid) vary with time for one fixed location at the top (crest) of the initial dune profile. Positive velocity is flooding conditions from ocean to bay. Maximum water velocities are near the location for largest gradients in water depth. The ratio of suspended sediment to total sediment transport rates, q_s/q_t is shown in Figure 12 for a representative test case. Around 5000 time step, the flow reverses (flood to ebb) so that the zero water flow rate also produces zero sediment transport. The bed-load accounts for roughly two-thirds of the total sediment transport.

Finally, as an example, Figure 13 displays the total sediment transport rate, q_t calculated at the dune crest (initial position) as a function of time for several time lags. Clearly, the longer time lags between maximum ocean and bay storm-surge elevations produce greater magnitudes in *both* the positive (flooding) and negative (ebbing) flow conditions.

Volume Conservation Tests

It is a desirable property that the solution of the finite-difference equation for sediment transport satisfy the overall mass-balance equation. Let V_i be the total volume of an initial barrier island and ocean/bay profile, and V(t) be the calculated profile volume from the numerical model at time level, t. Then the cumulative volume change, ΔV_e in percent is defined as:

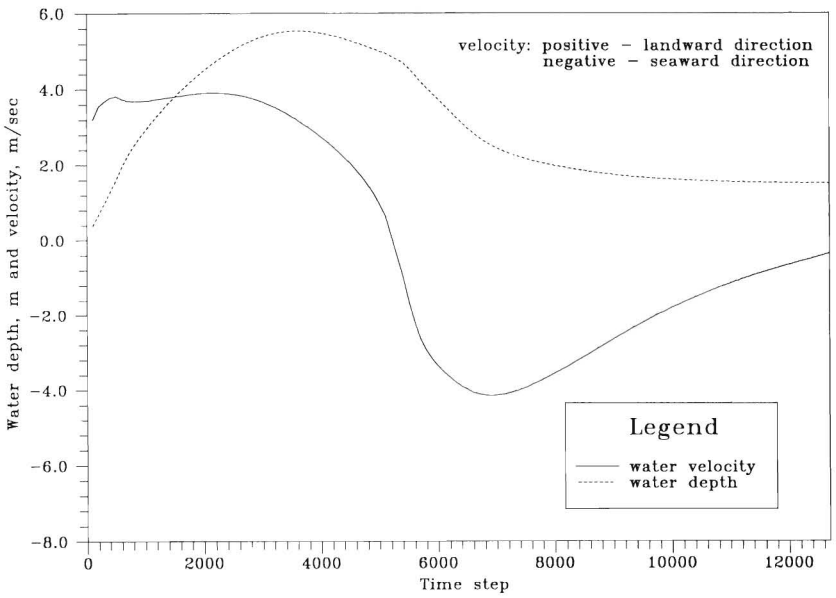

Figure 11. Water Depth and Velocity Variation at the Initial Top of the Dune. (h_{om}=4.0m, h_{bm}=3.0m, t_{lag}=3hr, D_{50}=0.3mm and Δt=4sec).

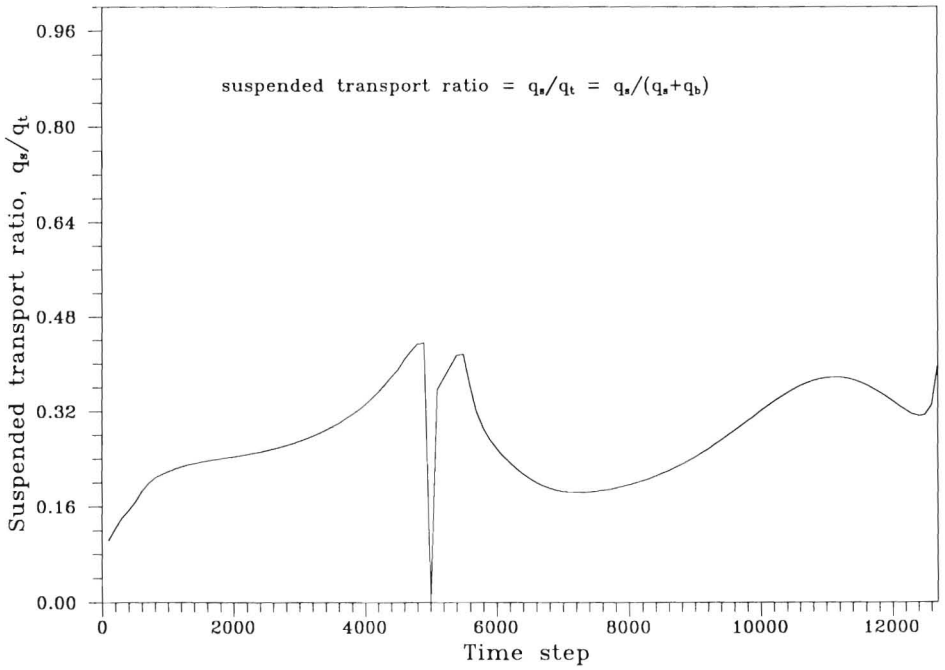

Figure 12. Suspended Sediment Transport Ratio at the Initial Top of Dune. (h_{om}=4.0m, h_{bm}=3.0m, t_{lag}=3hr, D_{50}=0.3mm and Δt=4sec).

$$\Delta V_e = \frac{S(t) - V(t)}{V_i} \times 100 \qquad (13)$$

where S(t) is the total volume of bottom profile above the datum over the computational domain at time level t and calculated from

$$\frac{dS(t)}{dt} = \frac{1}{(1-p)}[q_t(t, jj) - q_t(t, 1)] \qquad (14)$$

with porosity, p, and sediment transport rates at the left-hand side, q_t (t, 1) and right-hand side, q (t, jj) boundaries.

The range of cumulative volume change from numerical errors was on the order of ± 0.01–0.02 percent for all the tested combination of variables discussed below. The total volume loss over the computational domain was mainly the losses at both boundaries and the volume loss from numerical errors was considered negligible for these tests.

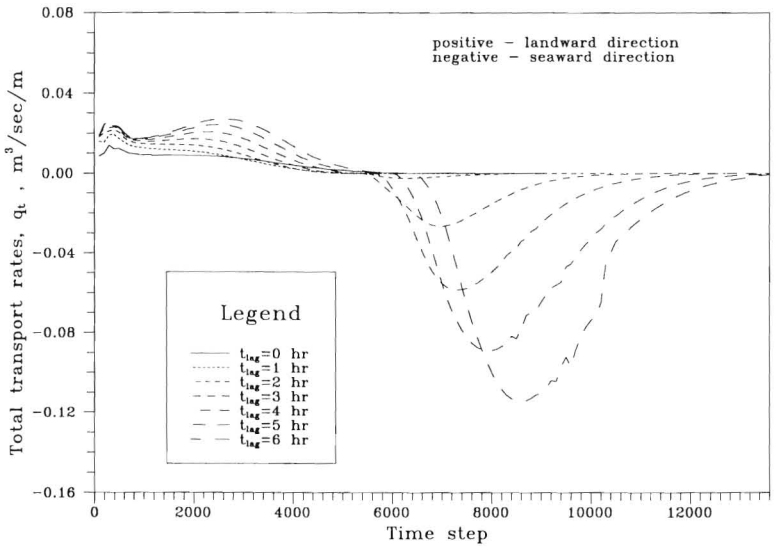

Figure 13. Total Sediment Transport Rates at the Initial Top of Dune. (h_{om}=4.0m, h_{bm}=3.0m, T=24hr, D_{50}=0.3mm and Δt=4sec).

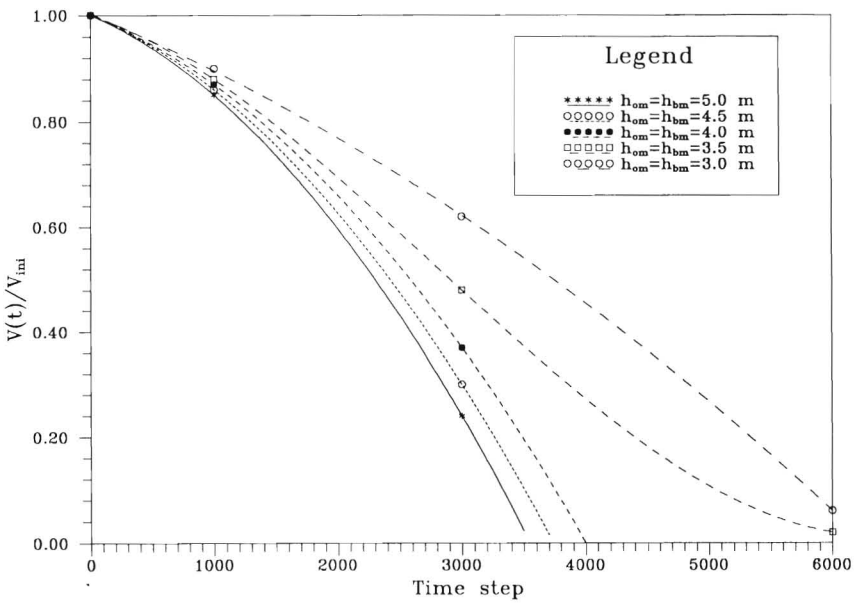

Figure 14. Volume Changes above MLLW for Five Different Storm Surge Levels. (t_{lag}=3hr, D_{50}=0.3mm and T=24hr).

ANALYSIS AND DISCUSSION OF TEST RESULTS

The following *independent* variables were found to be the key parameters for barrier island change during storm events.

- storm surge level at ocean and bay;
- time lag between maximum storm surge levels;
- sediment grain size; and
- storm duration.

The numerical model calculates the profile elevation, Z (x,t) for all grid points and time steps in the numerical simulation. To aid and simplify the analysis, the barrier island volume above MLLW is calculated along with the centroid position of this volume for each time step. And then, the barrier island (or dune) retreat speed can be found from the time rate of movement of the centroid position. Barrier island volume change above MLLW and retreat speed then become the key *dependent* variables that give a relatively simple, yet meaningful way to interpret the modeled results.

Storm Surge Level

Storm surge level is one of the most significant factors in determining profile change and barrier retreat rate. The peak surge level *difference* between ocean and bay determines the flow magnitude and direction over the whole computational domain.

The relative volume changes above MLLW for five different storm surge levels ($h_{om}=h_{bm}$) are shown in Figure 14 with the remaining variables held constant (t_{lag}=3.0hr, D_{50}=0.3mm and T=24hr). It is clear that higher storm surge levels more rapidly increase the barrier volume erosion rate. At time step 3000, the relative volume change at lower storm level ($h_{om}=h_{bm}$=3.0m) is about 0.62 but only 0.24 when h_{om} = h_{bm} = 5.0m. This is further clarified in Figure 15 which shows the fastest dune retreat speeds (≈0.05m/sec) comes from the highest storm surge levels. Note that the dune retreat speeds level-off in time.

For different storm-surge levels (stage) between ocean and bay (constant time lag) it is generally found that the largest stage difference produces the largest volume change and fastest dune retreat rate.

Time Lag

The time lag in maximum storm surge levels between ocean and bay produces the hydraulic gradients that determine the flow direction. Time lags from zero to six hour were tested in the model. The maximum, six hour time lag is approximately equivalent to the time difference between high and low gravitational tide levels in the study area.

Figure 16 shows relative volume change (solid line, left axis) and dune retreat speed (dotted line, right axis) for seven different time lags at 1 hr increments. The barrier volume moves landward toward the bay about 400 to 500m for the shorter time lags (0.0–2.0hr) with significant erosion, but the barrier volumes remains *above* MLLW at the end of the simulations. However, for the longer time lags (3.0–6.0hr) the barrier volume is completely eroded below MLLW and a breach event occurs for the case shown (h_{om} = 4m, h_{bm} = 3m, D_{50} = 0.3mm, T = 24 hr). Eroded materials are transported by the water flows and deposited in the bay for shorter time lags (0–2.0 hr) and in the ocean for longer time lag (3–6 hr) simulations.

Sediment Grain Size

The six different grain sizes are investigated ranging from D_{50} = 0.1mm up to 1.0mm. Grain size is one model parameter

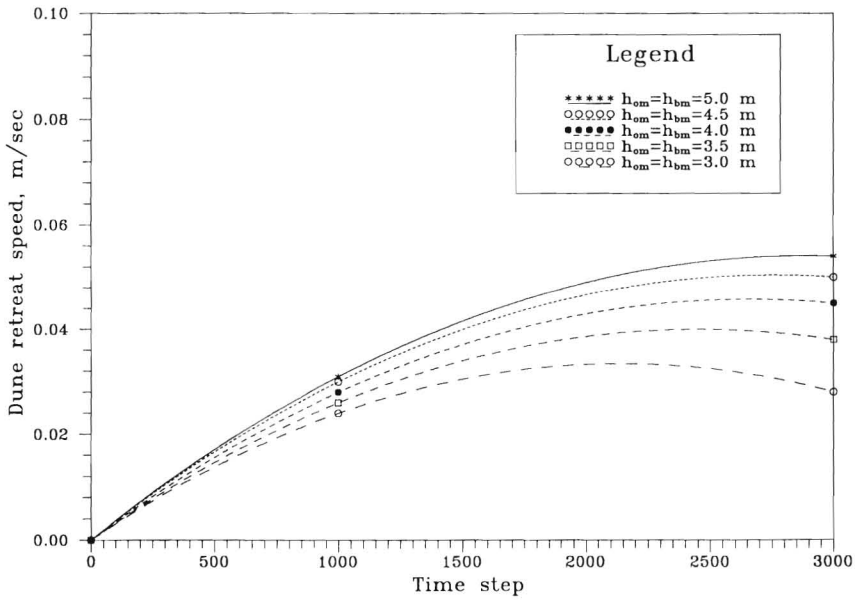

Figure 15. Dune Retreat Speeds for Five Different Storm Surge Levels. (t_{lag}=3hr, D_{50}=0.3mm and T=24hr).

that was found to significantly affect the movement of the centroid of the barrier volume. Figure 17 shows the relative volume change (solid line, left axis) and retreat speed (dotted line, right axis) for the range of median sand diameters tested. The smallest grain size, D_{50} = 0.1mm resulted in the least volume change and minimum retreat speed, which is perhaps intuitively opposite to what is expected. A middle range value, D_{50}=0.4mm give the fastest volume loss and maximum retreat speed. Larger particle size up to D_{50} = 1.0mm then showed a slower volume loss and retreat rate, as expected.

A possible explanation for these trends can be found by closer examination of the sediment transport formulas employed (VAN RIJN, 1984a , b). He assumed that the sediment transport rate can be described sufficiently accurately by two dimensionless parameters, a dimensionless particle parameter, D* and a transport stage parameter, T. The T-parameter

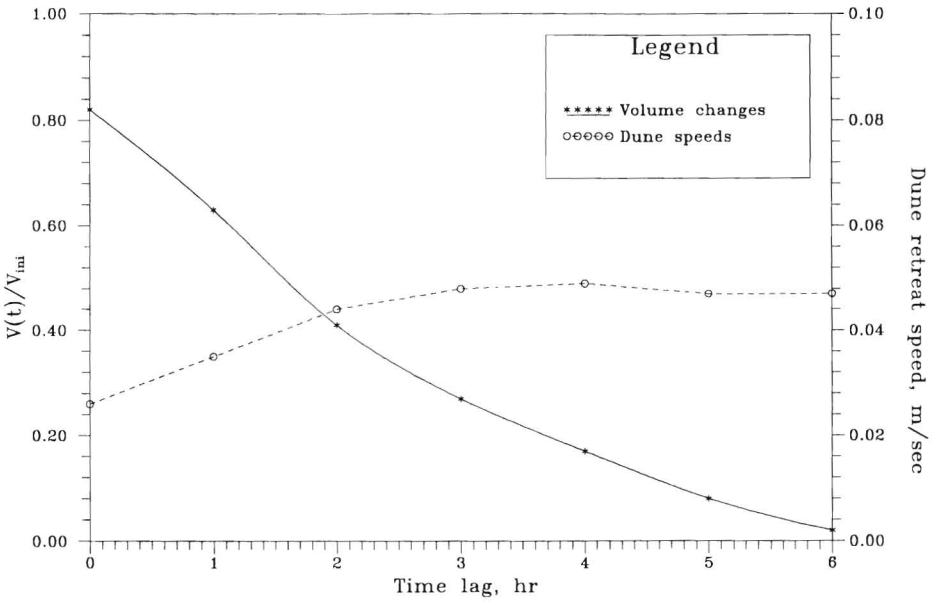

Figure 16. Volume Changes and Dune Retreat Speeds above MLLW for Various Time Lags at t=3000. (h_{om}=4.0m, h_{bm}=3.0m, D_{50}=0.3mm and T=24hr).

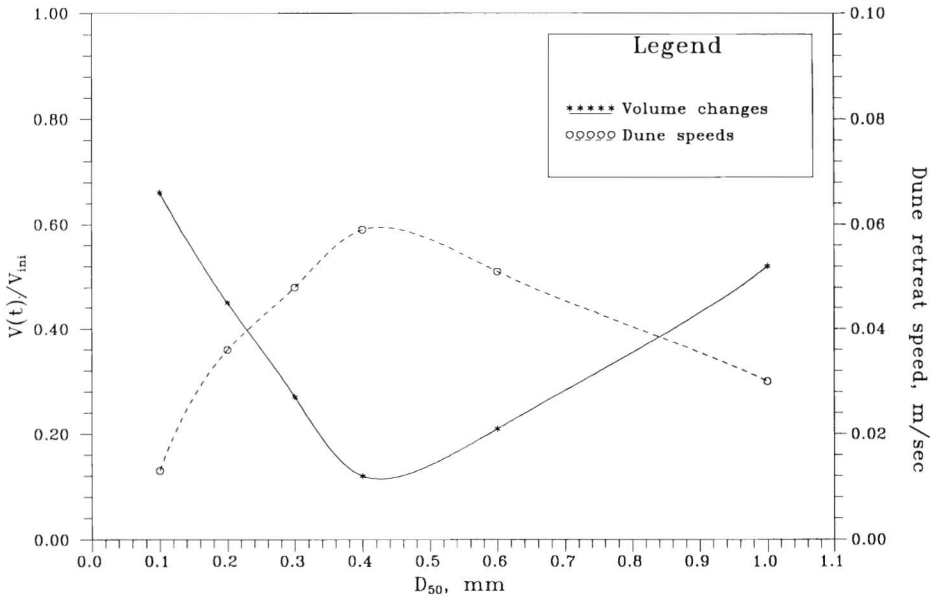

Figure 17. Volume Changes and Dune Retreat Speeds above MLLW for Various D_{50} at t=3000. (h_{om}=4.0m, h_{bm}=3.0m, t_{lag}=3.0hr and T=24hr).

expresses the mobility of the particles in terms of the "stage" of movement relative to the critical stage for initiation of motion as described by the Shields curve. On the Shields curve (VAN RIJN, 1984a), the minimum critical bed-shear velocity, which generally gives maximum sediment transport, occurs at $D_{50}\approx 0.4\sim 0.5$mm. The curve for volume change generally follows the Shields curve in a similar manner, so that these sensitivity tests of the numerical model for sand diameters can be considered to produce reasonable results.

Storm Duration

The water flow characteristics are strongly affected by the shape of the storm surge hydrograph. Peak surge level and storm duration control the hydrograph shapes modeled by equations (11) and (12). For a constant peak surge level, shorter storm durations produce more rapid changes in flow depth and velocity than longer duration storms. This is demonstrated in Figures 18 for relative volume change, $V(t)/V_i$.

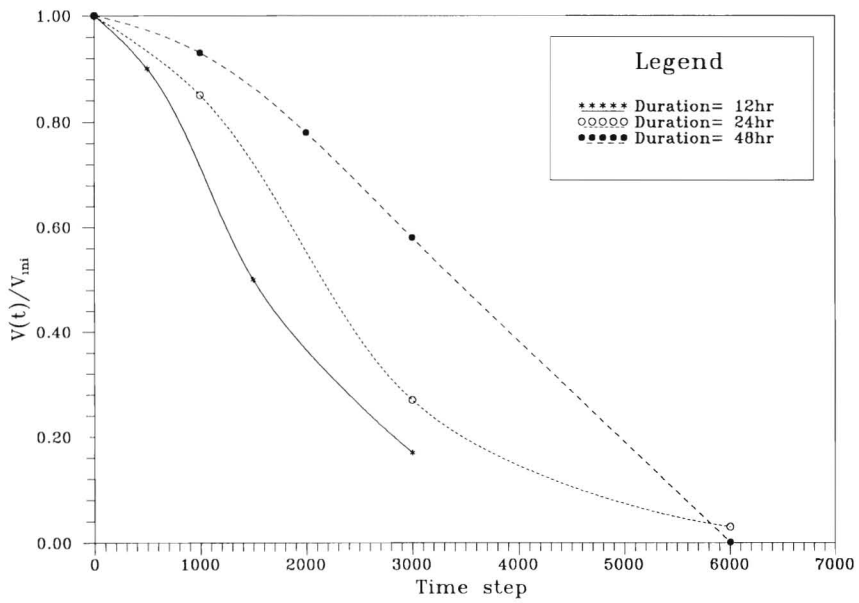

Figure 18. Volume Changes above MLLW for Various Storm Durations. (h_{om}=4.0m, h_{bm}=3.0m, t_{lag}=3.0hr and D_{50}=0.3mm).

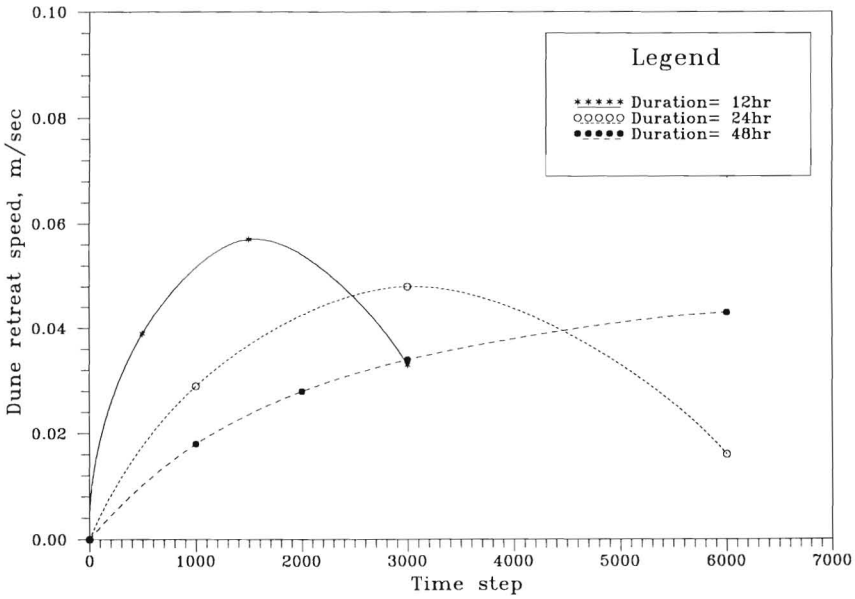

Figure 19. Dune Retreat Speeds above MLLW for Various Storm Durations. (h_{om}=4.0m, h_{bm}=3.0m, t_{lag}=3.0hr and D_{50}=0.3mm).

At the 3000 time step level, the longest duration storm tested (48 hr) produced about 0.6 relative change whereas only 0.2 of the initial volume remained for the shortest duration event (12 hr) tested. Figure 19 for retreat speed also shows that the shortest duration storm events produced the highest dune retreat speed of about 0.06 m/sec.

Barrier volumes above MLLW were completely eroded during these simulations in all cases (note t_{lag} = 3 hr). A shorter duration storm moves sediment to the ocean side and the longer duration storm distributes eroded sediment into the bay area. In the longer duration events, there are no distinct sediment flows from bay to ocean due to the relatively milder water flow characteristics. Because the hydraulic gradients between the ocean and bay in the shorter duration storms is much greater than over the longer duration, faster retreat speed and strong ebbing flows are created during the shorter duration storm events.

Volume Changes During Four Modeling Stages

Finally, the relative volume change, $V(t)/V_i$ for all four modeling stages covering almost 16 hours of simulation are shown in Figure 20 for a 24 hour storm event. (h_{om} = 4.0m, h_{bm} = 3.0m, t_{lag} = 3 hr, D_{50} = 0.3mm). In the SBEACH model (Stage I) for wave attack of the dunes, no significant volume loss above MLLW is shown because eroded volume from the dune crest is redistributed close to the foreshore and overwashed behind the dune crest. The maximum volume loss in percentage among all simulations during Stage I was 0.69 percent of initial barrier volume above MLLW. (Note that a considerable volume loss to the subaerial beach volume may occur during Stage I but that relative to the entire *barrier island* volume, this "loss" to the subaqueous beach profile is extremely small).

Stage II produces zero volume change. Almost all of the eroded barrier volume above MLLW comes from Stages III and IV due to the storm tidal flows across the island and subsequent sediment transports to the profile below MLLW on both the bay and ocean sides of the island. Wave action is not responsible for the breaching of barrier islands.

CONCLUSIONS AND RECOMMENDATIONS

Conclusions

We have been able to successfully link together four different numerical codes to simulate the combined effects of water wave attack followed by overland and tidal flows and sediment movements across a one-dimensional, barrier beach. Three of the models were newly developed for this study using finite-difference approximations of the conservation laws for open channel flow and sediment transport. One, existing model (SBEACH) was employed for initial stages of dune and beach erosion due to wave attack at elevated water level events. This initial stage proved to be of relative minor importance for a breach event so that very similar results would probably have been found using any one of many available models for stage one. The accuracy of the linked numerical models was examined through volume conservation tests and it was concluded that the combined models produced very little numerical error.

The relative volume change, centroid position and barrier retreat speed provide simple, yet meaningful indicators for the modeled results. For the range of physical parameters considered, we can draw the following conclusions from the numerical model tests.

(1) Peak surge level *difference* between ocean and bay boundaries regulates flow conditions and directions. Large hy-

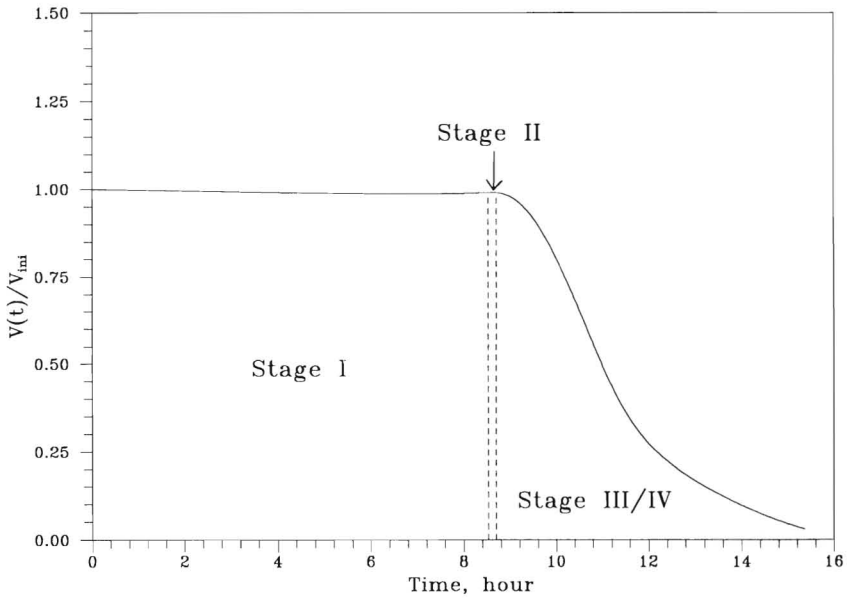

Figure 20. Volume Changes above MLLW in Each Stage for 24 Hours Storm Duration. (h_{om}=4.0m, h_{bm}=3.0m, t_{lag}=3.0hr and D_{50}=0.3mm).

draulic stage differences produce greater volume loss (above MLLW) and faster barrier retreat speed.

(2) Smaller time lags (< 2 hours) transport eroded sediments to the bay while larger time lags (>3 hours) carry eroded sediments into the ocean. Since most open barrier-bay systems (*i.e.* segmented barrier islands with many existing tidal inlets) have short time lags, eroded sediments are mainly transported to the bay side of the system. The actual time lag depends on the barrier breaching mode (inundated or localized, Figure 2), the distance from the existing to potential breach location and other factors. The one-dimensional model only gives some insight in this regard.

(3) Median grain size of 0.4mm produced maximum volume loss and retreat speed. Grain size was one model parameter that significantly influenced movement of the barrier centroid.

(4) Shorter duration storms produce strong ebbing flows and faster barrier retreat speeds because of stronger stage (head) gradients in time than longer duration storm events.

(5) In general, most sediments are transported landward into the bay by large peak storm surge differences with short time lags and longer duration storm events. And conversely, seaward sediment transport of barrier materials occurs for smaller peak storm surge differences with longer time lags and shorter storm durations.

(6) The numerical model for barrier island change has responded properly to each model variable and therefore we conclude that the model can produce reasonable, qualitative results, within the obvious limitations of the one-dimensional assumption.

RECOMMENDATIONS

Based on our experience with the one dimensional model, we offer the following recommendations.

(1) The bed form (ripples, bed dunes, etc.) influence on the boundary resistance term in the momentum equation for water flow in Stages III/IV should be investigated to determine the relative magnitude of change produced when compared to these plane bed results.

(2) Other geometric sections characterized by barrier width at MLLW, dune crest elevation(s), dune base width(s), etc., *i.e.* other barrier island initial volumes should be studied.

(3) Field data (bathymetry, topography, oceanographic, etc.) should be found for a breaching site and a calibration attempted. The case considered should be close to one-dimensional, if possible.

(4) A depth-averaged, two-dimensional (horizontal) model for combined water motion and sediment transport should be developed. Both the local breaching and inundated breaching models (Figure 2) should be investigated.

(5) Laboratory and field experimental data for the short term breach growth (width) should be incorporated in the development of the 2D model for the local breaching mode.

(6) The 2D model should be calibrated and verified with field data of breaching events for barrier islands.

LITERATURE CITED

ABBOTT, M.B., 1966. *An Introduction to the Method of Characteristics*. New York: American Elsevier.

ABBOTT, M.B., 1979. *Computational Hydraulics: Elements of the Theory of Free Surface Flows*. London: Longman Scientific and Technical, 425p.

ABBOTT, M.B. and BASCO, D.R., 1989. *Computational Fluid Dynamics*. London: Longman Scientific and Technical, 425p.

ACKERS, P. and WHITE, W., 1973. Sediment transport: new approach and analysis. *Journal Hydraulic Division*, (ASCE), 99, HY11.

ALLEN, J.R.L., 1970. The avalanching of granular solids on dune and similar slopes. *J. Geology*, 78(3), 326–351.

AUBREY, D.G. and WEISHAR, L. (eds.), 1988. *Hydrodynamics and Sediment Dynamics of Tidal Inlets*. Lecture Notes on Coastal and Estuarine Studies, Vol.29, New York: Springer-Verlag.

BASCO, D.R., 1977. On numerical accuracy in computational hydraulics. *Proc 25th Annual Hydraulics Division Specialty Conf.* (College Station, TX), pp. 179–186.

BATHURST, J.C.; GRAF, W.H., and CAO, H.H., 1987. Bed-load discharge equations for steep mountain rivers. *Sediment Transport in Gravel-Bed Rivers. In*: C.R. THORNE; J.C. BATHURST, and R.D. HEY (eds.), New York: Wiley.

CHEN, Y.H., 1973. Mathematical Modeling of Water and Sediment Routing in Natural Channels. Ph.D. Thesis, Colorado State Univ., Fort Collins, Colorado.

CHOW, V.T., 1957. *Open Channel Flow*. New York: McGraw Hill.

CORREIA, L.-R.P.; KRISHNAPPAN, B.G., and GRAF, W.H., 1992. Fully coupled unsteady mobile boundary flow model. *J. Hydraulic Engineering* (ASCE), 118, 3.

CUNGE, J.A.; HOLLY, F.M., and VERWEY JR, A., 1980. *Practical Aspects of Computational River Hydraulics*. London: Pitman.

DALLY, W.R.; DEAN, R.G., and DALRYMPLE, R.A., 1985a. Wave height variation across beaches of arbitrary profile. *J. Geophy. Research*, 90, (C6), 11917–11927.

DALLY, W.R.; DEAN, R.G., and DALRYMPLE, R.A., 1985b. A model for breaker decay on beaches. *Proc. 19th Conf. Coastal Engineering*, pp.82–98.

DEAN, R.G., 1976. Beach Erosion: Causes, processes, and remedial measures. *CRC Reviews in Environmental Control*, 6(3), 259–296.

DEAN, R.G., 1977. Equilibrium beach profiles: U.S. Atlantic and Gulf Coasts. Dept. Civil Eng., Ocean Eng. Rept. No.12, Univ. of Delaware, Newark, DE.

DOLAN, R.H., 1985. Sandbridge beach and back bay, Virginia. Tech. Rept. Coastal Research Assoc., Inc., Charlottesville, Virginia, 120p.

DOLAN, R.H. and LINS, H., 1987. Beaches and Barrier Islands. *Scientific American*, 255(7), 68–77.

EDELMANN, T., 1968. Dune erosion during storm conditions. *Proc. 11th Conf. Coastal Eng.* (London), pp.719–722.

EDELMANN, T., 1972. Dune erosion during storm conditions. *Proc. 13th Conf. Coastal Eng.*, (Vancouver), pp.1305–1312.

ENGELUND, F. and HANSEN, E., 1967. A Monograph on Sediment Transport. Copenhagen, Denmark: Technisk Forlag.

FREAD, D.L., 1974. Numerical properties of implicit four-point finite-difference equations of unsteady flow. National Weather Service, *TM HYDRO-18*, Washington, DC.

GIESE, G.S., 1978. The barrier beaches of Chatham, Mass. Rept., Provincetown Center for Coastal Studies.

HALLERMEIER, R.J., 1981. Seaward limit of significant sand transport by waves, US Army Corps of Engineers, Coastal Engineering Research Center, *Rept CETA 81-2*, WES, Vicksburg, MS.

HAVNØ, K. and BRORSEN, M., 1986. A general mathematical modeling system for flood forecasting and flood control. *Proc. International Conf. Hydr. Floods and Flood Control*, Cambridge, UK; BHRA, Stevenage.

HILL, J.R., 1981. Experiments with a Nonstaggered, Implicit, Finite-Difference Operator for the Two-Dimensional Free Surface Flow Equations. Unpublished MS thesis, Dept. of Ocean Eng., Texas A&M Univ., College Station, TX.

HOLLY, F.M., JR. and RAHUEL, J.-L., 1990. New numerical/physical framework for mobile-bed modeling. *J. Hydraulic Research*, 28(4), 401–416.

HSU, S.M. and HOLLY, F.M., JR., 1992. Conceptual bed-load transport model and verification for sediment mixtures. *J. Hydraulic Eng.*, 118(8), 1135–1152.

KRIEBEL, D.L. and DEAN, R.G., 1984. Beach and dune response to severe storms. *Proc. 19th Conf. Coastal Engineering*. (Houston), pp.1587–1599.

KRIEBEL, D.L. and DEAN, R.G., 1985. Numerical simulation of time-dependent beach and dune erosion. *Coastal Eng.*, 9, 221- 245.

LARSON, M. and KRAUS, N.C., 1989. SBEACH: numerical model for simulating storm-induced beach change. *Tech. Rept. CERC-89-9*, CERC, U.S. Army Eng. Waterway Exp. Sta., Vicksburg, MS.

LARSON, M.; KRAUS, N.C., and BYRNES, M.R., 1990. SBEACH: numerical model for simulating storm-induced beach change; Rept.2: numerical formulation and model tests. *Tech. Rept. CERC-89-9*, CERC, U.S. Army ENG. Waterway Exp. Sta., Vicksburg, MS.

LAX, P.D., 1954. Weak solutions of non-linear hyperbolic equations and their numerical applications. *Comm. Pure and Appl. Math.*, 17, 335–353.

LAX, P.D. and WENDROFF, B., 1960. System of conservation laws. *Comm. Pure and Applied Math.*, 13, 217–237.

LEATHERMAN, S.P., 1988. *Barrier Island Handbook*. Laboratory for coastal research, Univ. of Maryland, College Park, pp.63.

LEFFLER, M.W.; BARON, C.F.; SCARBOROUGH, B.L., and HATHAWAY, K.R., 1993. Annual data summary for 1991, CERC field research facility. U.S. Army Corps of Engineers, WES, CERC, *TR-CERC-93-9*.

LIGGET, J.A. and CUNGE, J.A., 1975. Numerical methods of solution of the unsteady flow equation, in *Unsteady Flow in Open Channels*, Vol.1, edited by Mahmood, K. and Yevjevich, V., Water Resources Pub., Fort Collins, Colorado.

LYN, D.A., 1987. Unsteady sediment-transport modeling. *J. Hydraulic Eng.* (ASCE), 113(1), 1–15.

MAHMOOD, K. and YEVJEVICH, V. (eds.), 1975. *Unsteady Flow in Open Channels*. Fort Collins, Colorado: Water Resources Publ.

MAHMOOD, K. and PONCE, V.M., 1976. Mathematical modeling of sedimentation transients in sand-bed channels. *Rept. CER75-76-KM-VMP28*, Eng. Res. Center, Colorado State Univ., Fort Collins, Colorado.

MOORE, B.D., 1982. Beach Profile Evolution in Response to Changes in Water Level and Wave Height. Unpublished MS thesis, Univ. of Delaware, Newark, Delaware.

PARK, I. and JAIN, S.C., 1986. River-bed profiles with imposed sediment load. *J. Hydraulic Eng.* (ASCE), 112, 4.

PARK, I. and JAIN, S.C., 1987. Numerical simulation of degradation of alluvial channel beds. *J. Hydraulic Eng.* (ASCE), 113(7).

PIERCE, J.W., 1970. Tidal inlets and washover fans. *J. Geology*, 78, 230–234.

PONCE, V.M.; INDLEKOFER, H., and SIMONS, D.B., 1979. The convergence of implicit bed transient models. *J. Hydraulic Div.* (ASCE), 105, HY4.

PREISSMANN, A., 1961. Propagation des intumescenes dans les canaux et rivieres. *1st Congress de l'Assoc. Francaise de Calcul Grenoble*, pp.433–442.

RAHUEL, J.L.; HOLLY, F.M.; CHOLLET, J.P.; BELLEUDY, P.J., and YANG, G., 1989. Modeling of riverbed evolution for bedload sediment mixtures. *J. Hydraulic Eng.* 115(11), 1521–1542.

RICHTMYER, R.D., 1963. *NCAR Tech. Note 63-2*, National Center for Atmospherics Research, Boulder, Colorado.

RICHTMYER, R.D. and MORTON, K.W., 1967. *Difference Methods for Initial Value Problems*. New York: Interscience.

VAN RIJN, L.C., 1984a. Sediment transport, part I: bed load transport. *J. Hydraulic Eng.* (ASCE), 110(10).

VAN RIJN, L.C., 1984b. Sediment transport, part II: suspended load transport. *J. Hydraulic Eng.* (ASCE), 110(11).

VAN RIJN, L.C., 1984c. Sediment transport, part III: bed forms and alluvial roughness. *J. Hydraulic Eng.* (ASCE), 110(12).

DE SAINT VENANT, A.J.C., 1871. Theory of unsteady water flow, with application to river floods and to propagation of tides in river channels. *French Academy of Science*, 73, pp.148–154,237–240.

SCHOONEES, J.S. and THERON, A.K., 1995. Evaluation of 10 cross-shore sediment transport/morphological models. *Coastal Engineering*, 25, 1–41.

SHIN, C.S., 1996. A One-Dimensional Model for Storm Breaching of Barrier Islands. Unpublished Ph.D. thesis, Old Dominion Univ., Norfolk, Virginia.

STEETZEL, H.J., 1993. Cross-Shore Transport During Storm Surges. Ph.D. Thesis, Delft University of Tech., Delft, The Netherlands.

SWART, D.H., 1976. Predictive equations regarding coastal transports. *Proc. 15th Conf. Coastal Eng.* (Honolulu), pp.1113–1132.

U.S. ARMY, 1989. *Beach Erosion Control and Hurricane Protection, Virginia Beach, Virginia. Phase II-General Design Memo.*, Vol.III, Corps of Engineers, Norfolk District Office.

VELLINGA, P., 1982. Beach and dune erosion during storm surges. *Coastal Engineering*, 6, 361–387.

VELLINGA, P., 1983. Predictive computational model for beach and dune erosion during storm surges. *Proc. Coastal Structures'83* (ASCE), pp. 806–819.

VOOGT, H.L.; VAN RIJN, L.C., and VAN DEN BERG, J.H., 1991. Sediment transport of fine sands at high velocities. *J. Hydraulic Eng.* (ASCE), 117(7).

DE VRIES, M., 1965. Considerations about non-steady bed-load transport. *Proc. 11th Congress, Int. Ass. of Hydraulic Res.*, 3, paper 3.8, Leningrad, USSR.

DE VRIES, M., 1973. River-bed variations-aggravation and degradation. *Delft Hydraulics Laboratory Publication No.107.*

WHITE, W.R.; MILLI, H., and CRABBE, C., 1973. *Sediment Transport: An Appraisal of Available Methods.* Hydrological Research Station, Wallingford.

WILSON, K.C., 1987. Analysis of bed-load motion at high shear stress. *J. Hydraulic Eng.* (ASCE), 113(1).

WILSON, K.C. and NNADI, F.N., 1990. Behavior of mobile beds at high shear stress. *Proc. 22nd Conf. Coastal Eng.* (Delft, The Netherlands).